

# An experimental study of flow over artificial bed forms

CS James<sup>\*1</sup> and CFG Cottino<sup>2</sup>

<sup>1</sup> Department of Civil Engineering, University of the Witwatersrand, Private Bag 3, WITS 2050, South Africa

<sup>2</sup>Mercurio Trade, PO Box 51401, Raedene 2124, South Africa

## Abstract

The boundary characteristics of flow over bed forms determine their behaviour and interaction with associated turbulent flow and sediment transport. The effects of bed-form geometry, surface roughness and discharge on boundary shear stress, pressure, water surface profile and separation length have been investigated experimentally at shallow (relative to bed-form height) flow depths. The length of separation zone was found to depend on the Froude number, grain roughness and bed-form geometry, and to be significantly greater than as measured previously at greater relative flow depths. Boundary shear stress is influenced strongly by discharge and bed-form geometry, and weakly by surface roughness.

## Introduction

Bed forms play an important role in the hydraulics of alluvial channels, being associated with both sediment transport and flow resistance. The turbulent flow, sediment transport and bed-form geometry constitute a mutually dependent system with continuous feedback interactions between the components. The complexity of the relationships in this "trinity" has been discussed by Leeder (1983), who warns against the treatment of any one component in isolation. The behaviour of the individual components is, however, little better understood at present than the interactions between them, and there is therefore some justification for investigating them independently. The understanding of processes in isolation that can be obtained through well-controlled experiments - even in highly artificial situations - provides a basis for developing an understanding of complex process interactions.

The boundary characteristics of the flow over a bed form, particularly the boundary shear stress, boundary pressure, and the length of separation zone, are important parameters in the flow - sediment transport - bed-form interaction. The boundary shear stress controls the movement of sediment grains and therefore determines the sorting of sediment on the bed-form surface, the rate of bed-load transport, and the bed-form geometry. It also determines the skin friction component of bed resistance. The distribution of pressure over a bed form determines the form resistance component of bed resistance. The length of separation determines the remaining area of bed over which skin friction is applied and therefore the relative importance of the resistance components. Engel (1981) has presented a discussion of the practical significance of the length of separation.

Progress has been made in the analytical description of these flow characteristics (e.g. McLean and Smith, 1986; Mendoza-Cabrales, 1987; Mendoza and Shen, 1990) and will be further advanced by continuing developments in computational fluid dynamics. Experimental and field measurements are also necessary, however, for validation and calibration of the analytical models

and for improving our understanding of the underlying physical processes. Various experimental studies have been reported. Laursen et al. (1962) measured distributions of velocity, pressure and boundary shear stress for air flow over triangular bed forms in a closed conduit. Raudkivi (1963) measured these characteristics as well as turbulence intensity for flow over a stabilised, natural ripple. Vanoni and Hwang (1967) measured velocity and pressure distributions over a stabilised ripple bed. Rifai and Smith (1971) conducted experiments with flow over a train of two-dimensional, smooth, triangular bed elements. On the basis of their measurements of velocity and turbulence intensity, they concluded that flow over triangular bed elements reproduces the essential characteristics of flow over alluvial dunes. Jonys (1973) measured pressure distributions and velocity profiles, from which he inferred boundary shear stresses, over naturally developed, unstabilised dunes. Vittal et al. (1977) conducted experiments on the flow of both water and air over a train of two-dimensional triangular bed elements. They used a fixed element height and a range of element lengths to study the effects of varying upstream slope on pressure and boundary shear stress distributions. They also examined the effects of surface roughness by coating the elements with sand grains for some experiments. Fehlman (1985) measured velocity, pressure and boundary shear stress distributions over smooth and roughened triangular bed elements with different flow conditions and a constant geometry.

Most experimental investigations of separation length have been conducted on downstream-facing vertical steps (e.g. Walker, 1961; Tani, 1957; Etheridge and Kemp, 1979). Chang (1970) used an iron angle section rather than a step. Raudkivi (1963; 1976) reports results for separation behind a stabilised ripple. Karahan and Peterson (1980) used streaming bi-refringence (the interpretation of velocity gradients from transmitted light interference patterns) to measure separation lengths for smooth dune-shaped beds with a constant geometry and for a range of flow conditions. Engel (1981) conducted a comprehensive set of tests on a downstream-facing vertical step and a train of idealised triangular dunes with different geometries and roughnesses. He produced a graphical predictor of the separation length as a function of dune height, length and sediment median grain size, based on his experimental results.

The experimental study reported here was carried out to extend the range of conditions investigated previously. Engel's (1981)

\* To whom all correspondence should be addressed.

☎ (011) 716-2568; Fax (011) 339-1762; E-mail csj@civen.civil.wits.ac.za  
Received 27 January 1995; accepted in revised form 27 July 1995.

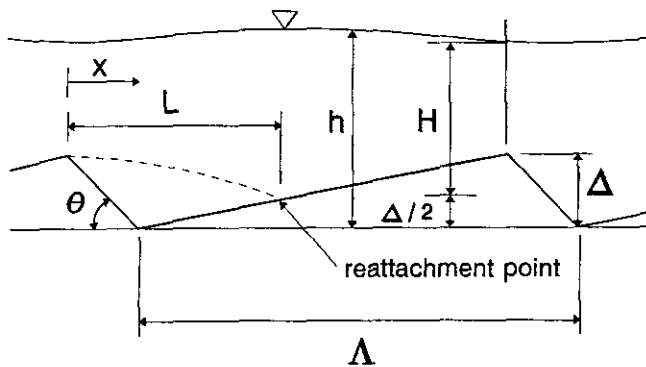


**Figure 1**  
Definition sketch for bed forms

		GEOMETRY			
		G1	G2	G3	G4
ROUGHNESS	S1		X		
	S2		X		
	S3	X	X	X	X
	S4		X		

**Figure 2**  
Combinations of geometry and surface roughness tested

TABLE 1 BED-FORM GEOMETRY AND ROUGHNESS DETAILS ( $\Delta = 45 \text{ mm}$ )		
Geometry	$\Lambda$ (mm)	$\Delta/\Lambda$
G1	750	0.06
G2	900	0.05
G3	1125	0.04
G4	1500	0.03
Roughness	$D_{50}$ (mm)	$D_{50}/\Delta$
S1	0.50	0.011
S2	0.93	0.021
S3	1.60	0.036
S4	3.05	0.068

experiments covered a wide range of geometries and grain roughnesses, but he has not presented pressure and boundary shear stress results. His experiments were also limited to flow depths greater than five times the dune heights, and results for shallower depths are needed (Davies, 1982). Vittal et al. (1977) used smooth surfaces and one grain-roughened surface in their experiments. The experiments described here were therefore designed to establish the effects, at relatively shallow flow depths, of bed-form geometry, surface roughness and discharge on the magnitudes and distributions of boundary shear stress and pressure, as well as on the water surface profile and separation length.

## Experimental apparatus and procedure

The experiments were conducted in a 380 mm wide glass-sided flume with a 9.0 m long tilting section, set at a slope of 0.002. Two-dimensional triangular bed forms (as shown in Fig. 1) were installed, extending across the full width of the flume and repeated identically to create a continuous train over the 9.0 m sloping section. Each bed form was constructed of galvanised metal sheeting attached to wooden supports. The bed forms were roughened by glueing on different grades of sand over which a very thin layer of varnish was applied by air gun.

Four different triangular shapes were tested. The maximum height ( $\Delta$ ) and downstream slope angle ( $\theta$ ) were kept constant at 45 mm and  $30^\circ$  respectively. The upstream slope was varied by using the base lengths ( $\Lambda$ ) listed in Table 1. For one of the shapes (G2) four different surface roughnesses were used, created with different sands for which the median ( $D_{50}$ ) sizes are given in Table 1. For the remaining shapes, only one roughness (S3) was used. These combinations of conditions enabled a systematic investigation of the effects of bed-form geometry and roughness on the flow characteristics to be conducted. The combinations of shape and roughness characteristics used in each series of experiments are shown in Fig. 2.

A range of flow conditions were applied to each of the shape-roughness combinations defined in Fig. 2. Boundary shear and pressure measurements were taken in each series of experiments for discharges ranging from 10  $l/s$  to 35  $l/s$  in increments of 5  $l/s$ . Separation lengths and water surface profiles were measured for discharges of 40  $l/s$  and 45  $l/s$  as well. A total of 55 experiments were conducted. All measurements were taken on the third bed form in the train, preliminary tests having shown that flow was fully established by this stage and that the flow characteristics being investigated were the same as for the bed forms immediately upstream and downstream. Further measurements were taken periodically on the fourth bed form during the experiments to ensure that the third one remained representative.

For each run the required flow condition was set and the discharge measured using a venturi meter in the supply line. Flow depths at two locations were monitored to ensure that flow was fully established before any measurements were taken. The water temperature was then recorded, followed by measurements of the water surface profile, the length of the separation zone, and the pressures and shear stresses on the bed. Water elevations, pressures and boundary shear stresses were measured at six equally spaced increments along the upstream slope of the bed form between the toe and crest points.

Water surface elevations were measured using a depth gauge with a vernier scale, fitted to a traversing mechanism mounted on a carriage on rails along the top of the flume. Elevations were measured along the centre line of the third bed form at the specified locations and also at the crest and toe of the fourth bed form, in

order to monitor relative uniformity of flow between successive bed forms.

The length of the separation zone was measured using the same simple visualisation technique as employed by Engel (1981). A potassium permanganate dye solution was injected with a syringe through a thin pipette mounted on the traversing mechanism. The position of the reattachment point at the end of the separation zone was located on both the third and fourth bed forms. The tip of the pipette was moved gradually towards the reattachment point until the dye stream indicated a change in local flow direction. This was done in both the upstream and downstream directions. The location of the reattachment point for each experimental condition was then taken as the average of the four measurements thus obtained.

The bed pressure was measured along the centre line of the third bed form using a piezometer tube mounted on the traversing mechanism and connected to a vertical manometer. Two tubes with different internal dia. (2.5 mm and 0.6 mm) were used for mutual checking.

Boundary shear stresses were measured using a 1.0 mm internal dia. pitot-static tube as a Preston tube, linked to a pressure transducer with an analogue display unit. This technique, in which boundary shear stress ( $\tau_0$ ) is determined from a single dynamic pressure measurement taken against the boundary ( $\Delta p = \rho v^2/2$ , where  $\rho$  is the water density and  $v$  is the local velocity), was first introduced by Preston (1954). The correlation between  $\tau_0$  and  $\Delta p$  is based on the existence of the logarithmic velocity profile near the boundary in turbulent flow. The detailed measurements of spatially accelerating flow over a triangular bed element by Cardoso et al. (1989) confirmed that a logarithmic profile persists within the inner flow region along the upstream inclined surfaces of the bed forms. The Preston tube technique is therefore appropriate for the conditions investigated, although it requires specific calibration. The calibration relationship for use with hydraulically smooth boundaries presented by Patel (1965) has been widely accepted. Calibrations for hydraulically rough boundaries are less reliable, however. Hwang and Laursen (1963) presented a relationship between  $\Delta p$  and  $\tau_0$  in terms of the tube dia., its position relative to the velocity profile datum, and the relative roughness of the bed. This relationship can be used directly for hydraulically rough turbulent flow, but for transitional flows it requires a correction which was not satisfactorily specified. Hollingshead and Rajaratnam (1980) presented a calibration chart for hydraulically smooth and rough boundaries, but this is not well corroborated by data in the transitional zone. Because of the uncertainties associated with existing calibrations in the transitional zone and the uncertain definition of bed roughness in terms of grain size, the relationship between  $\Delta p$  and  $\tau_0$  was calibrated specifically for the surfaces used in these experiments.

The calibration experiments were conducted in a 100 mm wide, 3.0 m long flume set to the same slope as the main flume. The bed was roughened with the four different sands in exactly the same way as for the triangular bed forms. Velocity profiles were measured at the centre line of each bed using the same pitot-static tube and pressure transducer as used for bed shear measurements. The reliability of this system was established by comparison with simultaneous velocity measurements taken with a propeller-type current meter. Velocity profiles were measured for each bed for near-bed velocities ranging from 0.12 m/s to 0.55 m/s, covering the range of values for the bed forms in the main experiments. Seven or eight profiles were measured for each of the four roughnesses. The average dynamic pressure against the bed was obtained from measurements at three locations, and the water temperature and

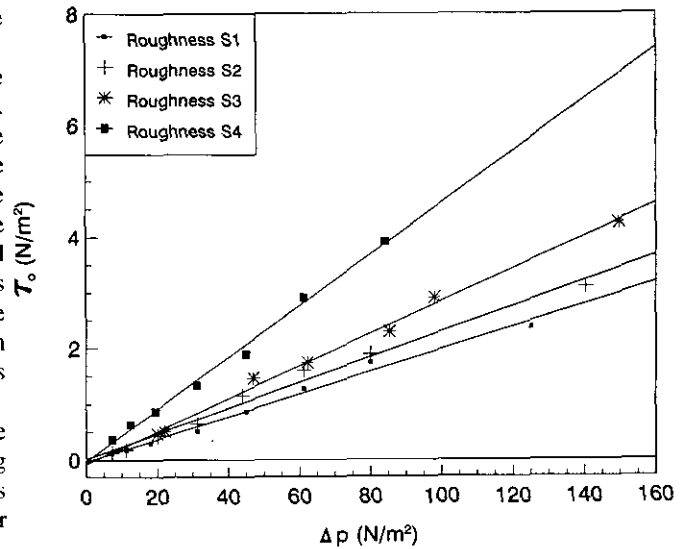


**Figure 3**  
Preston tube calibrations for different surface roughnesses

**TABLE 2**  
PRESTON TUBE CALIBRATION RELATIONSHIPS

Roughness	$\tau_0/\Delta p$
S1	0.0201
S2	0.0228
S3	0.0291
S4	0.0463

flow depth recorded. For each profile, velocity was plotted against the logarithm of height above the bed and  $\tau_0$  calculated from the gradient. The values of  $\tau_0$  and corresponding  $\Delta p$  are plotted for each bed roughness in Fig. 3. The correlation coefficient for each of the straight lines fitted to the data is 0.99. Ignoring the slight deviations from the origin, the relationships can be specified as listed in Table 2. All the velocity profiles and details of the calibration analyses are presented by Cottino (1993).

Using these calibrations, bed shear stresses were measured at the specified locations along the centre line of the third bed form and also along parallel lines 10 mm on either side of the centre line. The three readings for each location were averaged to minimise the effects of uneven roughness on the setting of the tube.

## Results

### Water surface profiles

In all the experiments the water surface profiles were invariably out of phase with the bed profile (Fig. 1), as expected for lower regime bed forms (dunes) which occur with subcritical flow. The water surface was smooth for the lower range of flows but developed irregularities at the higher flows, with greater variations in elevation. The profiles for different flow conditions for bed form type G2S3 are typical and are shown in Fig. 4. Generally, the smooth water

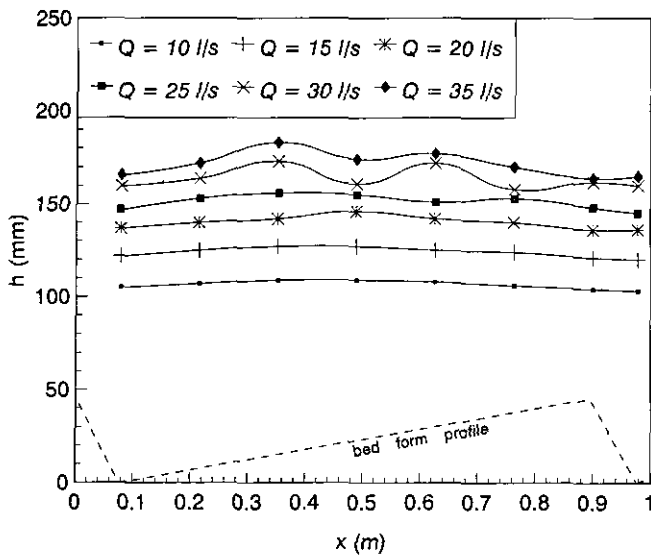


**Figure 4**  
Water surface profiles for bed form G2S3

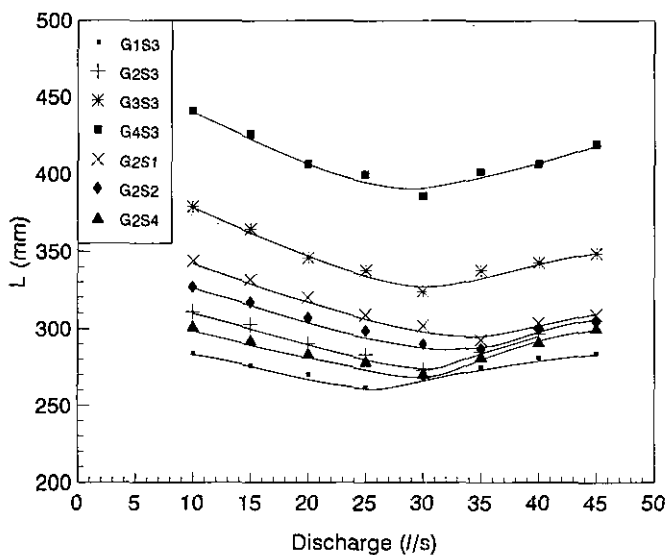


**Figure 5**  
Measured separation lengths for all experiments

surface profiles did not persist for Froude numbers ( $Fr$ ) greater than 0.45 ( $Fr = V/(gH)^{1/2}$ , where  $V$  is the average flow velocity and  $H$  is the average flow depth). The profiles at the higher flows were also associated with the sharp increases in boundary shear stress described later, suggesting that the hydraulic conditions are incompatible with the bed-form geometry and that the geometry would be modified by local erosion if it were not fixed. This is supported by the observation of Van Rijn (1984) that washing-out of dunes occurs at a Froude number of 0.6 in flumes.

The average flow depth is used in many alluvial channel relationships, as for example in the bed-form geometry descriptions of Van Rijn (1984) and Yalin (1977), and in the computation of flow velocity and Froude number. It is widely assumed that the average flow depth can be estimated as the flow depth at the dune crest plus half the height of the dune ( $H$ , as shown in Fig. 1) (e.g.

Engel, 1981; Engelund and Fredsoe, 1982; Shen et al., 1990). The water surface profiles measured in these experiments were used to calculate average flow depths for comparison with this estimate. The value of  $H$  was found to differ from the calculated average by an average of 2.8% over all the tests, with a maximum difference of 6.42%. This estimate is therefore considered to be reliable for practical purposes, and has been used in the analysis of the results of these experiments

### Length of separation zone

The measurements of the length of the separation zone ( $L$ ) are presented for all the experiments in Fig. 5. (The length is measured from the crest of a bed form to the reattachment point on the upstream slope of the following bed form (Fig. 1)). Figure 5 shows that the separation length varies with bed-form geometry, surface roughness and flow condition.

Through dimensional analysis and physical interpretation, Engel (1981) identified the important variables associated with the length of the separation zone. He proposed the general relationship

$$\frac{L}{\Delta} = f\left(\frac{\Delta}{\Lambda}, \frac{D_{50}}{\Delta}, \frac{H}{\Delta}, Fr\right) \quad (1)$$

In his experiments Engel found no dependence of  $L/\Delta$  on  $Fr$  and only weak dependence on  $H/\Delta$ , and he consequently simplified Eq. (1) by eliminating these variables. The present experiments reveal a distinct dependence on  $Fr$  (Figs. 6 and 7). The length of separation decreases with increasing  $Fr$  to a minimum in the region of  $Fr = 0.5$ , and it increases gradually thereafter. Karahan and Peterson (1980) also reported an inverse proportionality between the separation length and  $Fr$  at low values of  $Fr$  (less than about 0.25), but constant lengths over the range of  $Fr$  investigated here (0.35 to 0.6).

Because the flow in these experiments was controlled by the resistance of the bed, velocity and flow depth were not independent and it is not possible to separate the effects of  $Fr$  and  $H/\Delta$ . Comparison with Engel's (1981) results suggests, however, that  $H/\Delta$  has a significant influence on  $L/\Delta$ . In Fig. 8 the minimum values of  $L/\Delta$  for the different geometries with roughness S3 are compared with the values reported by Engel for a similar roughness. Considering that the ranges of  $Fr$ ,  $\Delta/\Lambda$  and  $D_{50}$  investigated by Engel and in these experiments, overlap considerably, the difference between Engel's and the present results is probably due to the different range of flow depths used. Here the range of  $H/\Delta$  was from about 1.7 to 3.5 whereas Engel specifies a lower limit of 5 in his conclusions and appears to have conducted experiments with values up to greater than 14. The lengths measured by Karahan and Peterson (1980) are more consistent with ours, but their flow depths are not reported.

The effect of grain roughness on separation length is shown in Fig. 6, which presents the results of all experiments with a common geometry (G2). This shows that the separation length reduces slightly as the grain roughness increases, which is consistent with the trend reported by Engel. The effect of grain roughness appears to be greater at the lower Froude numbers investigated; the curves tend to converge after the point of minimum separation length.

Figure 7 presents the results for experiments with constant grain roughness and varying geometry. This shows that the length of separation decreases as the bed form becomes steeper. This trend is similar to that found by Engel, although the actual values of  $L/\Delta$  are significantly higher. Unlike the effect of grain roughness, the effect of bed-form geometry appears to be independent of the

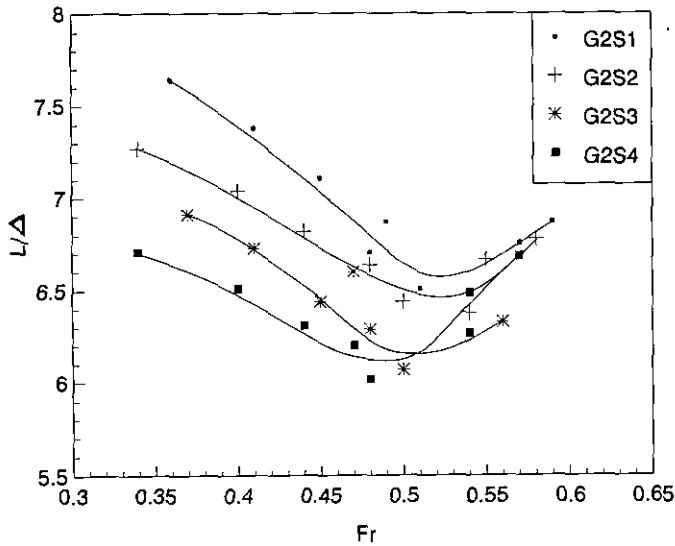


**Figure 6**  
Effect of Froude number and surface roughness on separation length

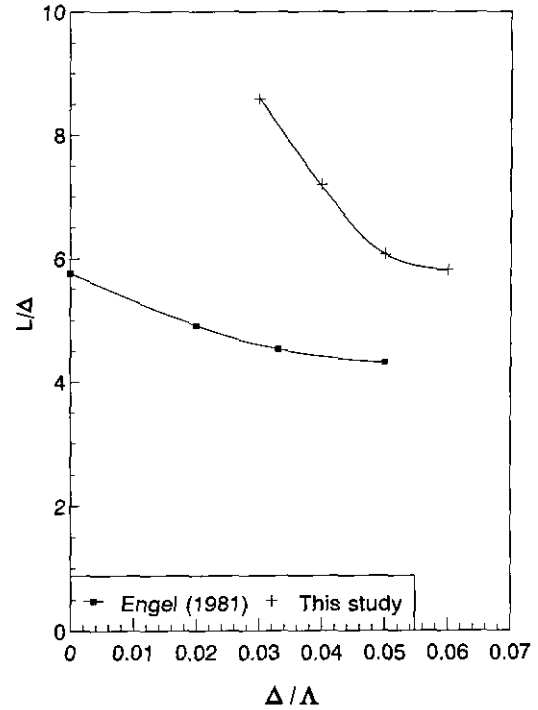


**Figure 8**  
Comparison of separation lengths with Engel's (1981) results

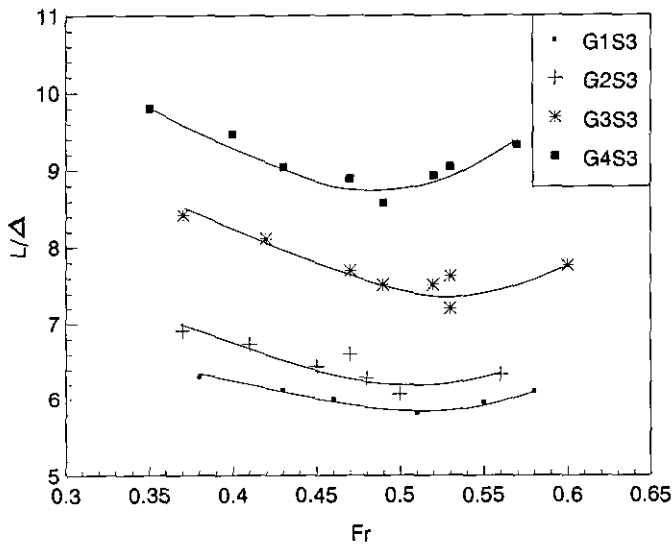


**Figure 7**  
Effect of Froude number and bed-form geometry on separation length

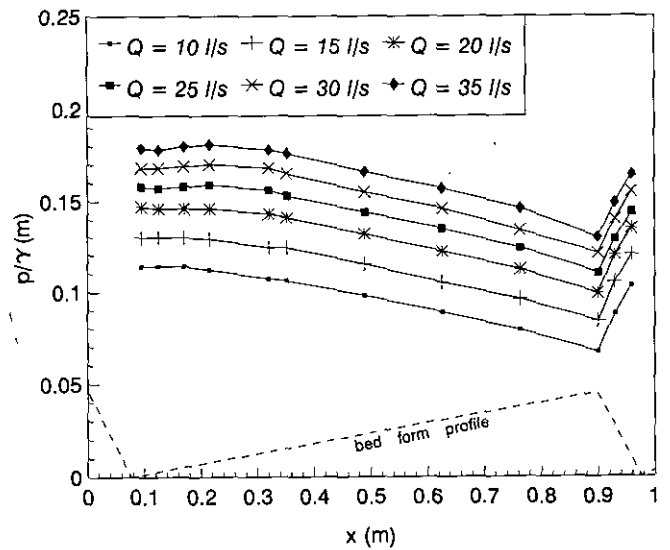


**Figure 9**  
Pressure distributions for bed form G2S3

Froude number.

Comparison of Figs. 6 and 7 suggests that the length of separation zone is influenced more by the bed-form geometry than grain roughness.

### Bed-pressure distributions

Bed-pressure ( $p$ ) distributions were measured for all experimental conditions and results are reported in full by Cottino (1993). The distributions for all flow conditions for the standard dune (G2S3) are shown in Fig. 9 and illustrate the typical profiles ( $\gamma$  is the specific weight of water). The pressure is constant within the separation zone along the upstream slope of the bed form, even though the bed elevation is increasing and the local flow depth is decreasing. Beyond the reattachment point the pressure begins to

decrease and continues to do so up to the crest, where it attains its minimum value. On the lee slope of the bed form the pressure increases rapidly as the flow depth increases, until it regains the maximum value at the toe. Very little variation of this pattern was observed with changing surface roughness.

### Bed shear stress distributions

The measured boundary shear stress distributions are presented for the different flow conditions for dune G2S3 in Fig. 10. Distributions

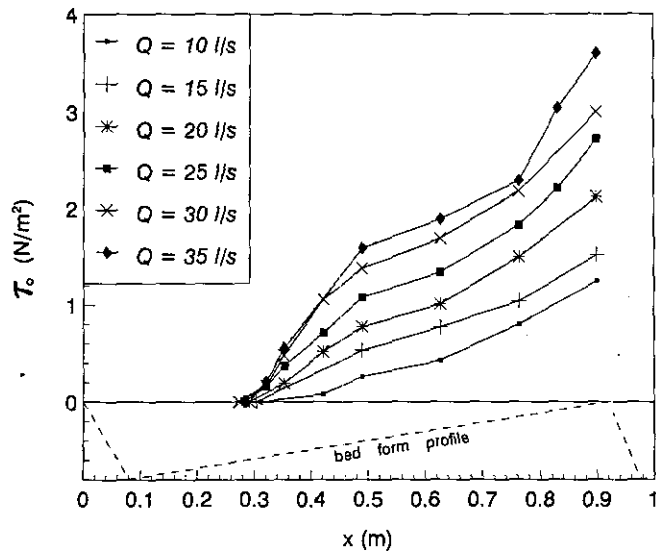


**Figure 10**  
Boundary shear stress distributions for  
bed form G2S3

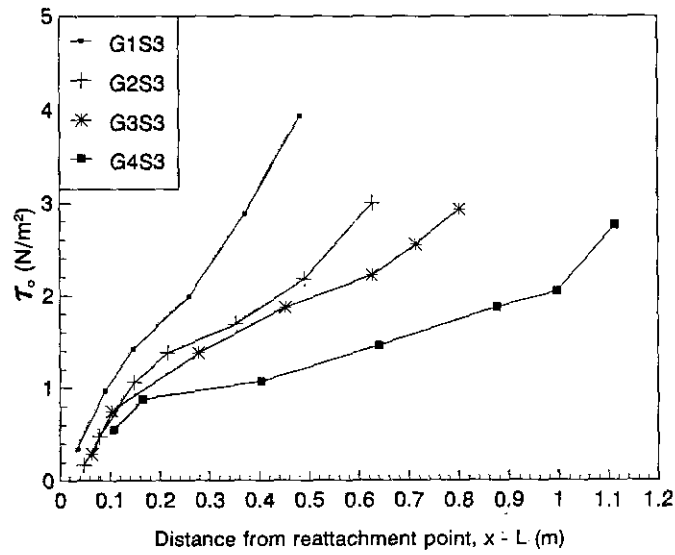


**Figure 11**  
Effect of bed-form geometry on boundary  
shear stress distribution

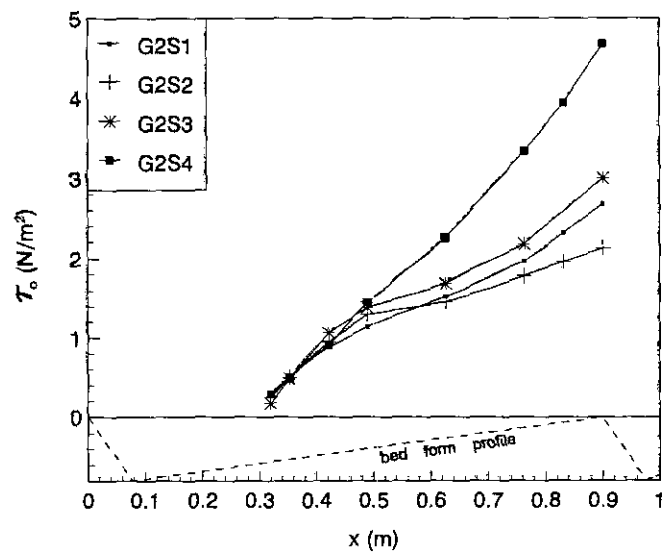


**Figure 12**  
Effect of surface roughness on boundary  
shear stress distribution

for the other bed forms show similar characteristics. In all cases  $\tau_o$  increases from zero at the reattachment point to a maximum at the crest, as observed also by Jonys (1973), Vittal et al. (1977) and Fehlman (1985). The profile shapes vary with flow condition, however, and are similar to the typical profile presented by Vittal et al. (1977) (for example) for some conditions only.

In general, four distinct regions can be identified on the measured profiles (Fig. 10):

- Within the separation zone the shear stress is effectively zero. Although no measurements were taken within the separation zone in these experiments, previous work (e.g. by Mendoza-Cabrales, 1987) has established this.
- Immediately downstream of the reattachment point there is a rapid increase in  $\tau_o$  from zero.
- The rapid increase is followed by a more gradual increase over most of the length of the upstream slope. This is almost linear for the lower discharges but becomes progressively more concave downwards as the discharge increases.
- At higher discharges there is also an accelerated increase in  $\tau_o$  over the last third of the length of the upstream slope towards the maximum value at the crest.

The transition between the second and third regions probably has the same origin as the local maximum in  $\tau_o$  reported by Fredsoe (1982), although no maxima were observed in these experiments. The observed increase in boundary shear stress towards the bed form crest would most likely cause a change in the bed-form geometry if the bed forms were not rigid, with increased erosion near the crest. This would lead to a flattening of the upstream slope which would be more natural than the triangular shapes used. It is probable that this shape adjustment would eliminate the exaggerated  $\tau_o$  values near the crest and that natural distributions are typified by those measured for low to intermediate discharges.

The growth of  $\tau_o$  is affected significantly by the bed-form geometry. Figure 11 shows the shear stress distributions beyond the reattachment points for the four geometries with common grain roughness, all at a discharge of 30 U/s. The rate of increase of  $\tau_o$ , particularly after the first region, clearly increases with increasing steepness.

Grain roughness size has less effect on the magnitudes and distributions of  $\tau_o$  (Fig. 12), except that values for the largest roughness (S4) were considerably greater than for the other roughnesses. For this roughness there is little difference between the regions of the profile identified above. The profiles for the smoother surfaces are not significantly different from each other and do not show a consistent trend in position.

## Conclusions

The average flow depth over a dune bed is reliably represented by the flow depth at the dune crest plus half the dune height.

The length of separation zone downstream of a bed form is very different at relatively low flow depths ( $1.7 < H/\Delta < 3.6$ ) from that reported by Engel (1981) at higher depths ( $5 < H/\Delta < 14$ ). In the lower range the separation length is also dependent on the Froude number, in contrast to Engel's results, exhibiting a minimum at a value of about 0.5. The separation length decreases with increasing grain roughness, particularly at low values of Froude number, and with increasing bed-form steepness.

The boundary shear stress on the upstream slope of the bed form increases from zero at the reattachment point to a maximum at the crest. The increase is rapid initially, followed by a region

of more gradual increase, and a further rapid increase towards the crest. The rate of increase is proportional to the surface slope. Measured shear stresses were highest for the roughest surface but no consistent trend was apparent for the other roughnesses.

## References

- CARDOSO, AH, GRAF, WH and GUST, G (1989) Spatially accelerating flow in smooth open channel. *Proc. Tech. Session A : Turbulence in Hydraulics - International Association of Hydraulic Research, XXIII Congress : Hydraulics and the Environment*. Ottawa, Canada.
- CHANG, FFM (1970) Ripple concentration and friction factor. *J. Hydraul. Div. ASCE* **96**(HY2) 417-430.
- COTTINO, CFG (1993) An Experimental Study of Flow around Bed Forms. Unpublished M.Sc.(Eng.) Thesis, University of the Witwatersrand, Johannesburg, South Africa.
- DAVIES, TRH (1982) Length of flow separation over dunes. Discussion. *J. Hydraul. Div. ASCE* **108**(HY7) 884-885.
- ENGEL P (1981) Length of flow separation over dunes. *J. Hydraul. Div. ASCE* **107**(HY10) 1133-1143.
- ENGELUND, F and FREDSOE, J (1982) Sediment ripples and dunes. *Ann. Rev. Fluid Mech.* **14** 13-37.
- ETHERIDGE, DU and KEMP, PH (1979) Velocity measurements downstream of a rearward facing step with reference to bed instability. *J. Hydraul. Res.* **17**(2) 107-119.
- FEHLMAN, HM (1985) Resistance Components and Velocity Distributions of Open Channel Flows over Bedforms. Unpublished M.S. Thesis, Colorado State University, Fort Collins, Colorado, USA.
- FREDSOE, J (1982) Shape and dimensions of stationary dunes in rivers. *J. Hydraul. Div. ASCE* **108**(HY8) 932-947.
- HOLLINGSHEAD, AB and RAJARATNAM, N (1980) A calibration chart for the Preston tube. *J. Hydraul. Res.* **18**(4) 313-326.
- HWANG, L-S and LAURSEN, EM (1963) Shear measurement technique for rough surfaces. *J. Hydraul. Div. ASCE* **89**(HY2) 19-37.
- JONYS, CK (1973) An Experimental Study of Bed Form Mechanics. Unpublished Ph.D. Thesis, University of Alberta, Edmonton, Alberta, Canada.
- KARAHAN, ME and PETERSON, AW (1980) Visualization of separation over sand waves. *J. Hydraul. Div. ASCE* **106**(HY8) 1345-1352.
- LAURSEN, EM, ADAMS, JR, HWANG, LS and CHEN, CL (1962) Pressure and Shear Distribution on Schematic Dunes. Technical Report No. 2, Civil Engineering Department, Michigan State University, East Lansing, Michigan, USA.
- LEEDER, MR (1983) On the interaction between turbulent flow, sediment transport and bedform mechanics in channelized flows. *Special Publications, Int. Assoc. Sediment.* **6** 5-18.
- McLEAN, SR and SMITH, JD (1986) A model for flow over two-dimensional bed forms. *J. Hydraul. Eng.* **112**(4) 300-317.
- MENDOZA, C and SHEN, HW (1990) Investigation of turbulent flow over dunes. *J. Hydraul. Eng.* **116**(4) 459-477.
- MENDOZA-CABRALES, C (1987) Refined Modelling of Shallow, Turbulent Flow over Dunes. Unpublished Ph.D. Thesis, Colorado State University, Fort Collins, Colorado, USA.
- PATEL, VC (1965) Calibration of the Preston tube and limitations on its use in pressure gradients. *J. Fluid Mech.* **23**(1) 185-208.
- PRESTON, JH (1954) The determination of turbulent skin friction by means of pitot tubes. *J. Royal Aeronaut. Soc. London.* **58** 109-121.
- RAUDKIVI, AJ (1963) Study of sediment ripple formation. *J. Hydraul. Div. ASCE* **89**(HY6) 15-33.
- RAUDKIVI, AJ (1976) *Loose Boundary Hydraulics* (2nd edn.) Pergamon Press (Inc.), Elmsford, New York.
- RIFAI, MF and SMITH, KVH (1971) Flow over triangular elements simulating dunes. *J. Hydraul. Div. ASCE* **97**(HY7) 963-976.
- SHEN, HW, FEHLMAN, HM and MENDOZA, C (1990) Bed form resistance in open channel flows. *J. Hydraul. Eng.* **116**(6) 799-815.
- TANI, L (1957) Experimental investigation of flow separation over a step. *Proc. Symp. Int. Union Theor. Appl. Mech. Boundary Layer Res. Freiburg/BR.* 26-29.
- VANONI, VA and HWANG, LS (1967) Relation between bed forms and friction in streams. *J. Hydraul. Div. ASCE* **93**(HY3) 121-144.

VAN RIJN, LC (1984) Sediment transport, Part III: Bed forms and alluvial roughness. *J. Hydraul. Eng.* **110**(12) 1733-1754.

VITTAL, N, RANGA RAJU, KG and GARDE, RJ (1977) Resistance of two-dimensional triangular roughness. *J. Hydraul. Res.* **15**(1) 19-36.

WALKER, GR (1961) A Study of Two-dimensional Flow of Turbulent Flow past a Step. Unpublished M.Sc. Thesis, University of Auckland, Auckland, New Zealand.

YALIN, MS (1977) *Mechanics of Sediment Transport* (2nd edn.) Pergamon Press, Braunschweig, Germany.

---